ARCHER

Collaborative Project (CP)

Co-funded by the European Commission under the Euratom Research and Training Programme on Nuclear Energy within the Seventh Framework Programme

Grant Agreement Number : 269892

Start date : 01/02/2011 Duration : 48 Months
www.archer-project.eu

Data Map to describe the Deposition Behaviour of Dust after Obstacles and in Dead End Volumes

Authors : M. LUSTFELD (TUD) , C. Stoeckel (TUD), W. Lippmann (TUD)

ARCHER - Contract Number: 269892
Advanced High-Temperature Reactors for Cogeneration of Heat and Electricity R&D
EC Scientific Officer: Dr. Panagiotis Manolatos

Document title	Data Map to describe the Deposition Behaviour of Dust after Obstacles and in Dead End Volumes
Author(s)	M. LUSTFELD (TUD) , C. Stoeckel (TUD), W. Lippmann (TUD)
Number of pages	18
Document type	Deliverable
Work Package	WP 23
Document number	D23.24
Issued by	TU Dresden
Date of completion	26/01/2015
Dissemination level	Confidential, only for members of the consortium (including the Commission Services).

Summary

Graphite dust generation and transport inside the primary coolant circuit is a significant safety issue in Pebble Bed High Temperature Reactors. Objective of this task is to analyse the dust deposition behaviour on metallic surfaces under as it was observed in High Temperature Reactors. The Experiments were performed in the small open loop flow channel Gas Particle Loop (GPLoop) at Helmholtz-Zentrum Dresden-Rossendorf under a range of flow conditions. The formation of single layer and multilayer deposits were observed. The experiments and the results are described in this deliverable.

Approval

Date	By
26/01/2015	Karl VERFONDERN
27/01/2015	Norbert KOHTZ
27/01/2015	Steven KNOL

Distribution list

Name	Organisation	Comments
P. Manolatos	EC DG RTD	Through the EC participant portal
All beneficiaries	ARCHER	Through the private online workspace

Table of contents

1 Introduction

Graphite dust production in the primary circuit is a significant safety issue in High Temperature Reactors, particularly in the pebble bed configuration [1]. In case of a Depressurized Loss of Forced Coolant accident (DLOFC), radioactively contaminated graphite dust can be remobilized from the deposition sites and blown out of the primary circuit and in the worst case across the reactor system boundaries. This would contribute to the radioactive source term of such an accident possibly above legal limits. Additionally, graphite dust deposition in primary circuit components such as heat exchangers can lead to a degradation of their performance. Therefore, thorough simulations on the graphite dust transport in HTR primary circuits are carried out by numerous research groups in order to determine the amount of particles that can be remobilized under accident conditions [2]. Based on these results, retention systems for dust particles can be designed.

To simulate the deposition of dust inside the primary coolant circuit, generic data for the particle transport are needed. The particles found in former HTRs and produced by experiments with a pebble mill [3] exhibit a flake-like shape and may therefore behave differently from what would be expected based on CFD simulations of the transport of spherical particles. .

2 Particle production and characterization

The production of graphite dust particles by friction between fuel pebbles was experimentally investigated by use of the small generic test facility *pebble mill*. Both the pebble type and the relative velocity and acting force on the contact surface between the pebbles were varied. After each experiment the generated dust was observed by means of laser scanning microscopy (KEYENCE VK-9700) and characterized. Hence the distribution of particle size and shape was determined. Detailed description of these experiments can be found in the deliverables D23.21 to D23.23.

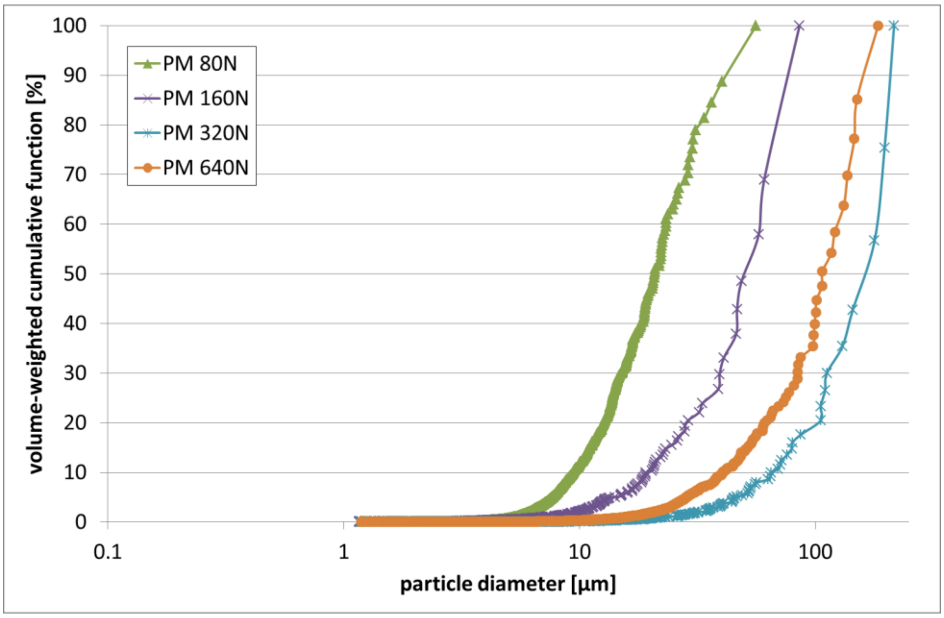

Figure 1: Volume-weighted particle size distribution of the dust generated by the pebble mill (PM) at different contact forces (80 N to 640 N)

The particle size distribution of the produced dust is shown as a function of the pebble contact force in Figure 1. In general, the higher the contact force, the larger are the particles. However, it has to be considered that the resolution of the laser microscope is limited and its sensitivity with respect to small particles is lower than that with respect to larger particles. Particle characterisation was done two-dimensionally. Thus, the generated data needs to be considered as indicative of the particle size to be expected in HTR primary circuits. Future experiments should be modified with two major objectives: Pebble abrasion under conditions closer to HTR primary circuit conditions, particularly higher temperature and high-purity helium atmosphere, and higher accuracy of particle characterization requiring particle analyser equipment that was not available within this work.

Furthermore, within the experiments only a small amount of particles was generated which was not enough as input for large-scale deposition experiments. Therefore, industrially produced graphite dust was used instead. Figure 2 shows the particle size distribution of the industrial graphite dust of type 23061 (Thielmann Graphite) used in these experiments (measured by laser diffraction spectrometry (HELOS/KR-H2487, Sympatec GmbH)) in comparison with particles found in the THTR-300 prototype reactor [4].

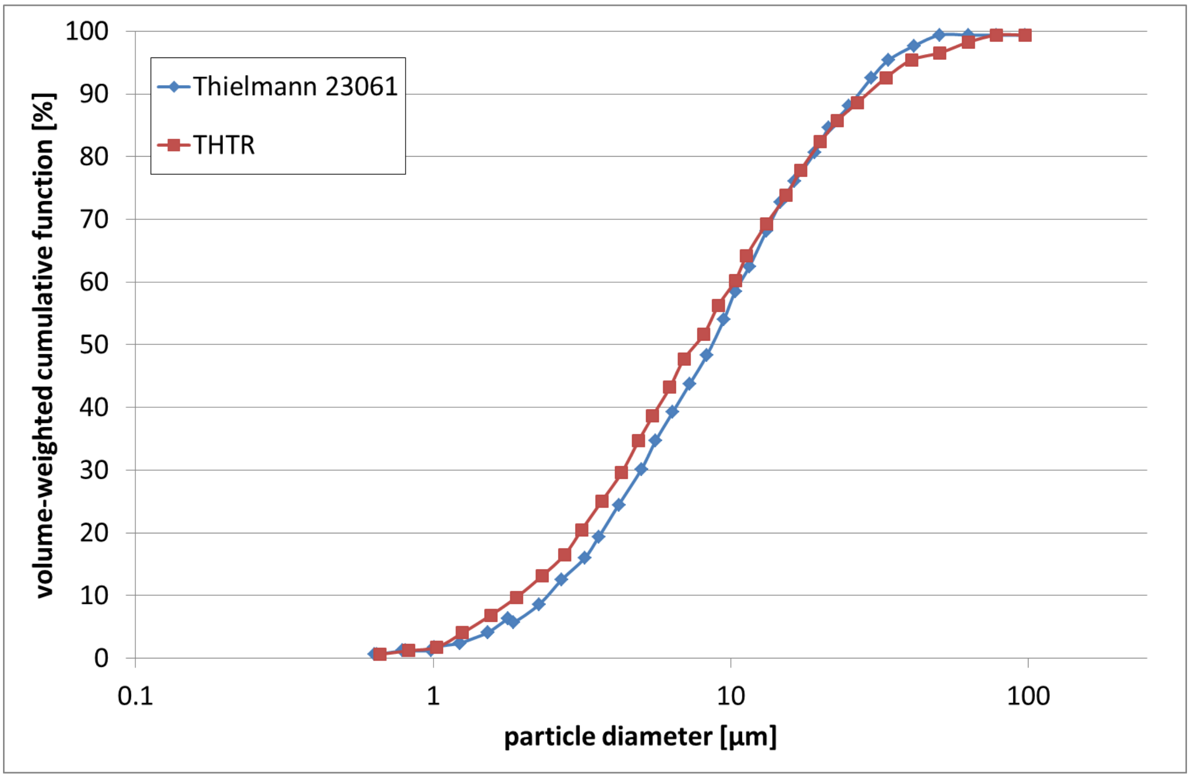

Figure 2: Volume-weighted particle size distribution of Thielmann type 23061 graphite in comparison to dust found in the THTR-300 reactor

The graphs exhibit a very similar trend. Therefore it is concluded that the type 23061 graphite could be used as an adequate substitute for typical HTR dust for the dust deposition experiments.

3 Particle deposition experiments

3.1 Principles of particle transport and deposition

To describe particle-fluid and particle-wall interactions, the following dimensionless characteristic numbers were used:

- The Reynolds number Re to specify the type of flow. It is a function of the relative velocity u, kinematic viscosity of the fluid ν and a characteristic length l. The characteristic length has to be chosen accurately depending on the flow phenomena which should be studied.

$$Re = \frac{u * l}{\nu} \qquad \text{Eq. 1}$$

- The Knudsen number Kn, which indicates whether the particle motion inside the flow heavily depends on fluid viscosity or, on the contrary, is rather moving like a molecule of the fluid itself. It is defined by the mean free path of the fluid λ and the characteristic diameter of the particle d.

$$Kn = \frac{2 * \lambda}{d} \qquad \text{Eq. 2}$$

- The mean free path can be calculated as follows [5]

$$\lambda = \frac{R * T}{\sqrt{2} * \pi * d^2 * p * N_A} \qquad \text{Eq. 3}$$

where R is the gas constant, T the fluid absolute temperature, p the absolute pressure and N_A the Avogadro constant.

- The particle relaxation time τ_p to describe the timescale a particle needs to adapt to a changing fluid velocity vector. It depends on the particle diameter d and particle mass density ρ_p, the kinematic viscosity of the fluid μ and a particle shape correction defined by the Cunningham correction factor C_c.

$$\tau_p = \frac{\rho_p * {d_p}^2 * C_c}{18 * \mu} \qquad \text{Eq. 4}$$

- The Stokes number St to describe the interaction of particles with a changing flow velocity vector due to tube bends or flow obstacles.

$$St = \frac{\tau_p * u}{l_o} \qquad \text{Eq. 5}$$

For a Stokes number St << 1 particles typically follow the streamlines of the flow, whereas for St >> 1 a collision between particles and any flow obstacles has to be expected.

- The particle deposition velocity u_d to quantify the deposition behaviour. It is defined as the ratio of particle mass flux per area J to the particle concentration inside the flow C.

$$u_d = \frac{J}{C} \qquad \text{Eq. 6}$$

For the typical design data of the HTR-Modul-Reactor the characteristic numbers are given in Table 1. These are compared to characteristics of air flows at ambient conditions, corresponding to the experimental conditions in GPLoop.

Table 1: Typical characteristics for HTR flow conditions and experiments at ambient air

	HTR-Modul	**ambient air**
temperature [°C]	700	20
pressure [MPa]	6	0.1
kinematic viscosity [m²/s]	15.4×10^{-6}	15.2×10^{-6}
mean free path [nm]	26	68
flow profile	turbulent	turbulent
Knudsen number D_p = (0.1 .. 50) µm	$10^{-3} – 5 \times 10^{-1}$	10^{-3} – 1.4
Particle relaxation time [s] D_p = (0.1 .. 50) µm	$4.4 \times 10^{-8} – 6.7 \times 10^{-3}$	$1.3 \times 10^{-7} – 1.7 \times 10^{-2}$

It can be seen that the characteristic numbers for particle transport and deposition are of the same order of magnitude for both HTR-conditions and air at ambient conditions. This implies that some particle transport properties in a HTR primary circuit can be expected to be similar to those in GPLoop. Also the Knudsen number indicates that the small particle fractions are in the transition regime between molecular and continuum flow. The particle relaxation time for air differs by a factor of about 3 from Helium suggesting that the particles in the air will follow the flow not as closely as in helium.

3.2 Flow channel

Dust deposition experiments were performed in the open loop flow channel Gas Particle Loop (GPLoop). In Figure 3 the basic design with the main components is shown: inlet with HEPA filter, flow formation zone and test section with rectangular cross section of 10 x 10 cm², diffusor, electrostatic precipitator and radial blower for flow generation.

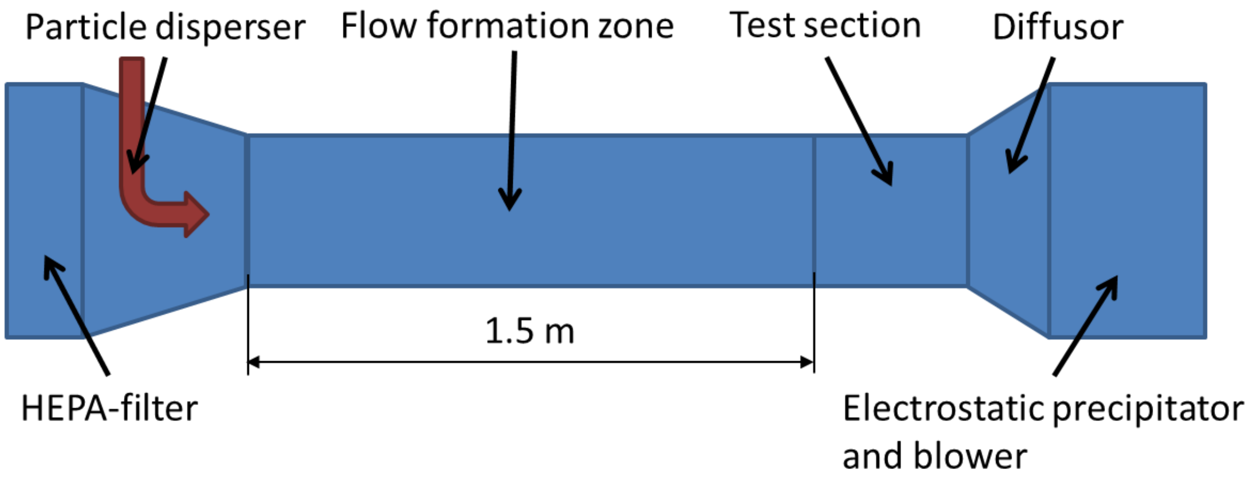

Figure 3: Illustration of the components of GPLoop with a cross section of 0.1 x 0.1 m²

The floor of the test section was particularly designed to allow the mounting of different samples and test geometries with a smooth transition to the flow formation zone. To avoid the influence of electrostatic forces on the particle the ground of the test section was electrically grounded.
The particle injection was provided in front of the flow formation zone to achieve a good dispersion of the particles along the entire flow channel. For single particle deposition experiments the dust disperser SAG410U (Topas GmbH) was used. In this case, both the aerosol disperser and the sample were heated up to 50 °C to avoid the influence of moisture on particle adhesion. The multilayer deposition was performed with the rotation brush generator RBG 1000 (Palas GmbH).

3.3 Single layer particle deposition

Initially a single layer particle deposition experiment was performed. The graphite particles were dispersed with the SAG410U into the flow with a Reynolds number of $19.9 \cdot 10^3$, based on the cross section geometry. The test section floor sample was an Alloy 617 blank sheet which was previously polished to achieve a smooth surface. Particles were dispersed for 1 minute into the flow to obtain enough particles on the surface for subsequent analyses. The blank sheet with the deposit was analysed by means of laser scanning microscopy and the particle size distribution was determined based on these images. Figure 4 shows the number-weighted size distribution of the dispersed particles investigated by both laser scanning microscopy and laser diffractometry and of the deposited particles on the metal sheets.

Firstly, a deviation between the two graphs of the dispersed particles can be seen which is caused by the different measurement techniques. Secondly, the curve of the deposited particles is biased to bigger particle fractions. It seems that larger particles deposit more easily on the floor than smaller ones. That effect may be caused by the gravitational force. Similar observations were made by Sehmel [6] who observed the motion of particles of 7 different size distributions inside an air flow with different Reynolds numbers.

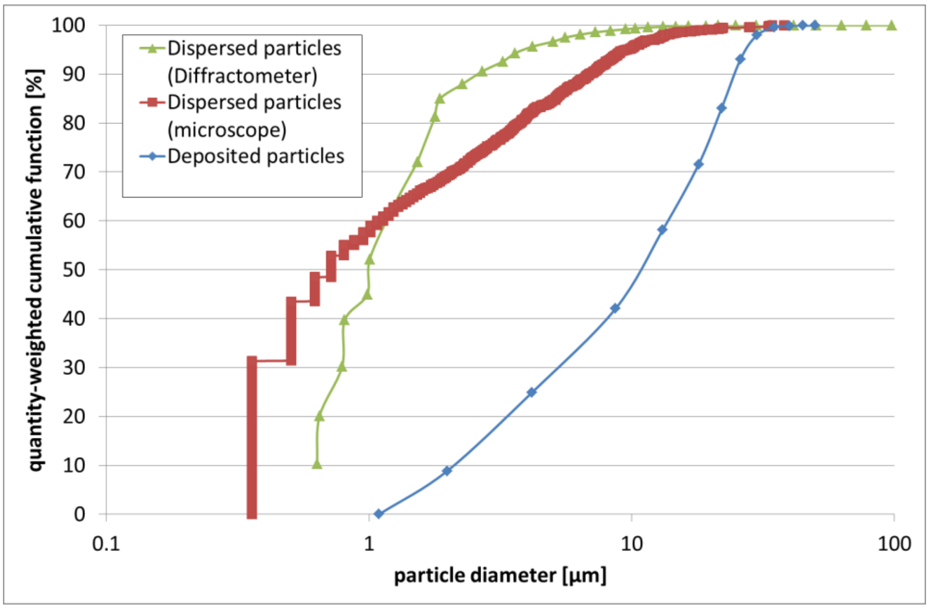

Figure 4: Particle size distribution of dispersed and settled dust for a single layer experiment at Re = 19.9*10^3

3.4 Multilayer particle deposition

3.4.1 General procedure

To perform the multilayer deposition experiments the test set up was modified. In order to investigate particle deposition at a flow obstacle a step was installed in the test section. Preliminary experiments had been performed to identify a representative flow obstacle shape that would yield enough particle deposition for subsequent analyses. It was found that particle deposition was much more efficient upstream than downstream of the step, Therefore, particle deposition was solely evaluated upstream of the step, equivalent to experiments regarding a “Forward Facing Step” (FFS) in the literature. The geometry of the modified test section is shown in Figure 5. The step height δ_s was 10 mm.

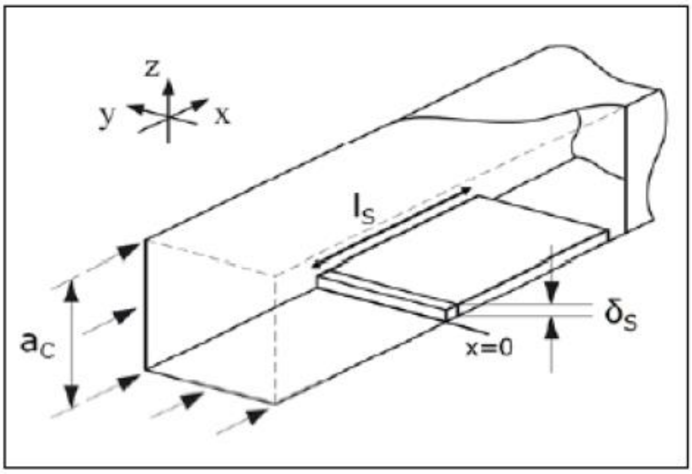

Figure 5: Geometry of the rectangular test section with a_c the channel width and δ_s the step height of the FFS

Taking into account the test section geometry and the bulk velocity u_x provided by the blower frequency f_B the Reynolds numbers Re_s listed in Table 2 were obtained (with respect to the FFS).

Table 2 Horizontal bulk velocity and FFS-related Reynolds number Re_s for different blower frequencies

f_B [Hz]	u_x [m/s]	Re_s [-]
5	0.95	610
10	2.2	1420
15	3.5	2240
20	4.7	3030
25	5.5	3520
30	6.5	4190
40	9.3	6000

The knowledge of the bulk velocity and the particle size distribution allows to calculate the expected Stokes numbers. With Figure 6 showing the cumulative function for the dispersed particle Stokes number it has to be assumed that an increase in the Reynolds number leads to an increase of particles colliding with the obstacle since St is increasing with Re. From this perspective, the difference between air at ambient conditions and helium at HTR primary circuit conditions does not seem to be prohibitively high for comparisons between flow channel and primary circuit results.

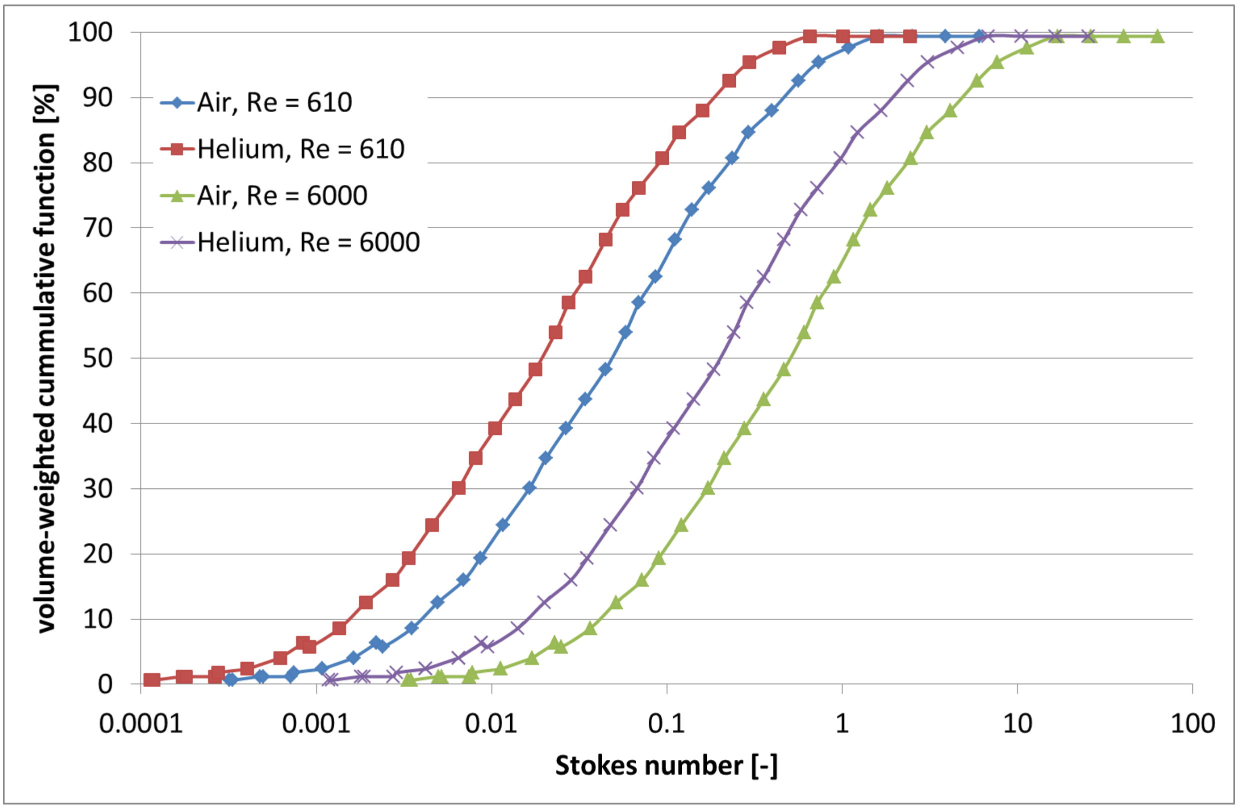

Figure 6 : Cumulative function of particle Stokes numbers for Reynolds numbers of 610 and 6000 for air at ambient and helium at HTR conditions

The particle dispersion was performed with the RBG 1000 with a maximum feed rate of 330 g/h, leading to a particle concentration C in the flow as shown in Table 3. It has to be considered that the concentration is based on the volume flow inside the channel and therefore is independent of the step height.

Table 3 Reynolds numbers and corresponding particle concentrations in the flows under investigation

f_B [Hz]	u_x [m/s]	C [g/m³]
5	0.95	9.6
10	2.2	4.2
15	3.5	2.6
20	4.7	2.0
25	5.5	1.7
30	6.5	1.4
40	9.3	1.0

The particle concentration is about 6 orders of magnitude higher than detected in the AVR which was estimated to be 5 µg/m³ [1]. Assuming that particles do not interact among each other no matter how high the particle concentration, one hour of deposition experiment could thus simulate up to 45 years of AVR operation. However, it has to be considered that long term effects like sintering or chemical reactions as discussed by Fachinger et al. [7] were not accounted for.

Every 18 minutes the sample was removed from the test section and the layer thickness in front of the step was measured with a laser triangulation system based on an optoNCTD1302 sensor (MICRO-EPSILON GmbH). The sensor was positioned by a motorised traverse and a field of x = 0 - -80 mm and y = 10 – 90 mm with increments of Δx = 0.1 mm and Δy = 5 mm could be observed.

The procedure was repeated three times at t = (18, 36, 54) min. After the last run the deposited layer was removed from the sample and gravimetrically weighed.

3.4.2 Flow field characterization

Before carrying out deposition experiments the flow field in front of the FFS was observed by means of particle image velocimetry (PIV) with a Flow Master 2C2D System (LaVision GmbH). Di-ethyl-hexyl-sebacat (DEHS) droplets were used as tracer particles and were dispersed with a liquid aerosol generator Type 10F03 (Dantec Dynamics A/S). In order to understand the complex flow field around the step in all 3 directions, the flow was measured in different horizontal and vertical planes within the test channel. The measurements were performed at z = (5, 10, 15, 20, 25, 50) mm and y = (30, 50) mm. For each configuration 500 pairs of double images were taken to obtain the time averaged flow field.

Figure 7 shows the time averaged velocity component ux at Res = 4190 at z = 50 mm und y = 50 – 100 mm.

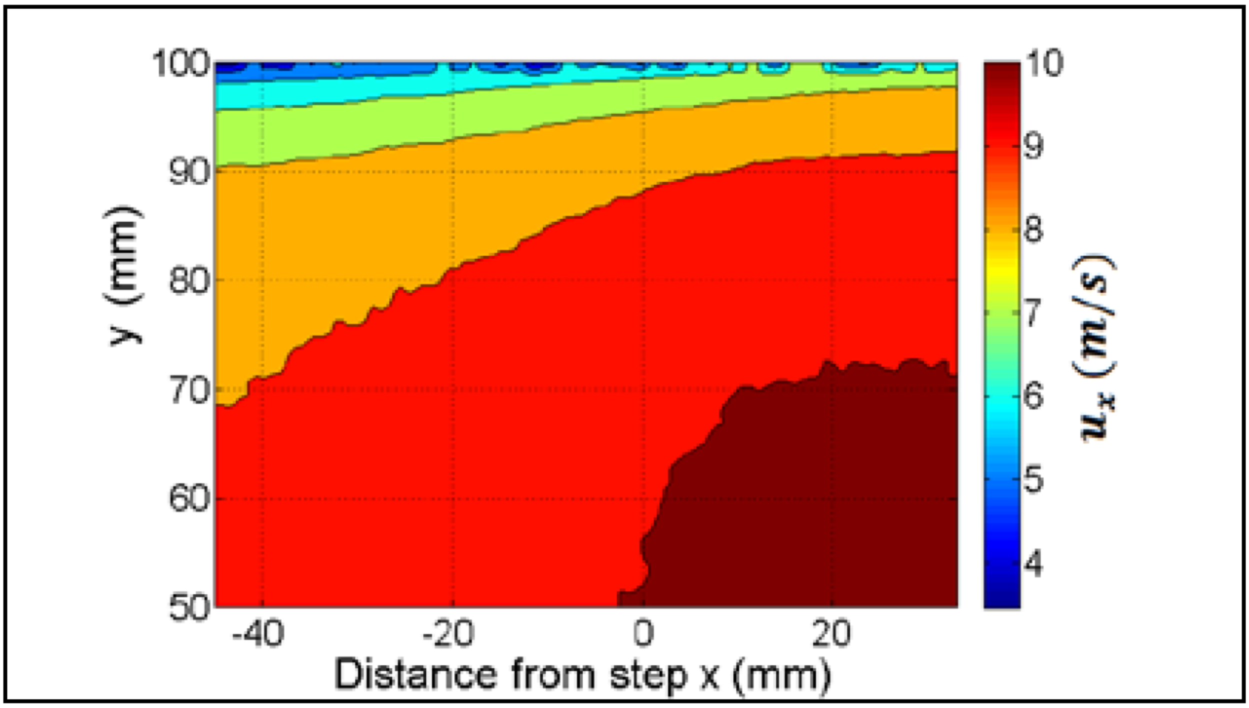

Figure 7 Horizontal flow component above the step in z = 50 mm plane

The horizontal section shows an increasing velocity over the step due to channel contraction by the FFS. In the vertical section the increasing velocity can also be seen. In front of the step a recirculation area is formed which can be characterized by its length l_{re}, height h_{re} and the absolute minimum velocity $u_{x,min}$ as shown magnified in Figure 8.

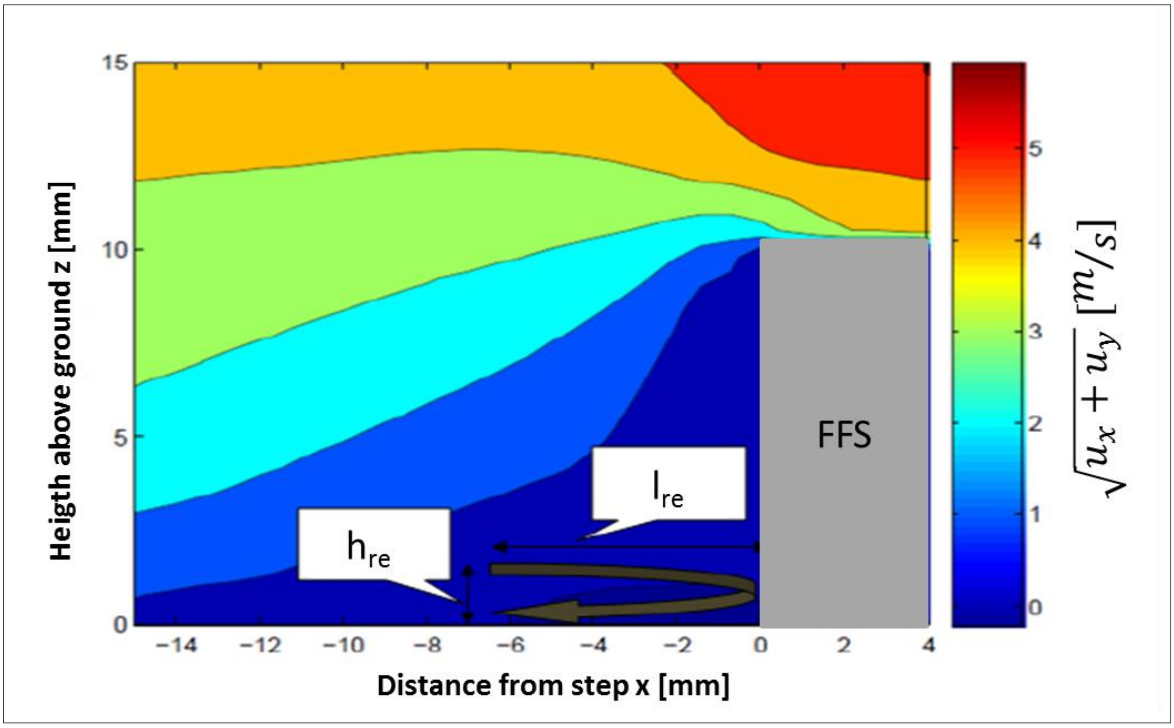

Figure 8 Magnified vertical plane of the flow field in front of the step at Re_s = 3030, illustrating the dimensions of the recirculation region

The corresponding recirculation characteristics are listed in Table 4.

Table 4 Characteristics of the recirculation area depending on the Reynolds number

Re_s [-]	l_{re} [mm]	h_{re} [mm]	$u_{x,min}$
610	15	2.5	-0.2
1420	5.5	1.3	-0.15
3030	5.0	1.2	-0.25
4190	4.5	1.1	-0.5
6000	3.5	1.0	-1.0

With increasing Reynolds number the area of the recirculation region decreases while the absolute value of the velocity $u_{x,min}$ in opposite direction of the mean flow increases. This agrees with the observations of Sherry *et al*. [8].

3.4.3 Multilayer height measurement

According to 3.4.1 after each 18 minutes of deposition the height of the settled dust was measured with a laser triangulation system. An exemplary evaluation of such a measurement can be seen in Figure 9 after a deposition time of t = 54 min at Re_s = 4190.

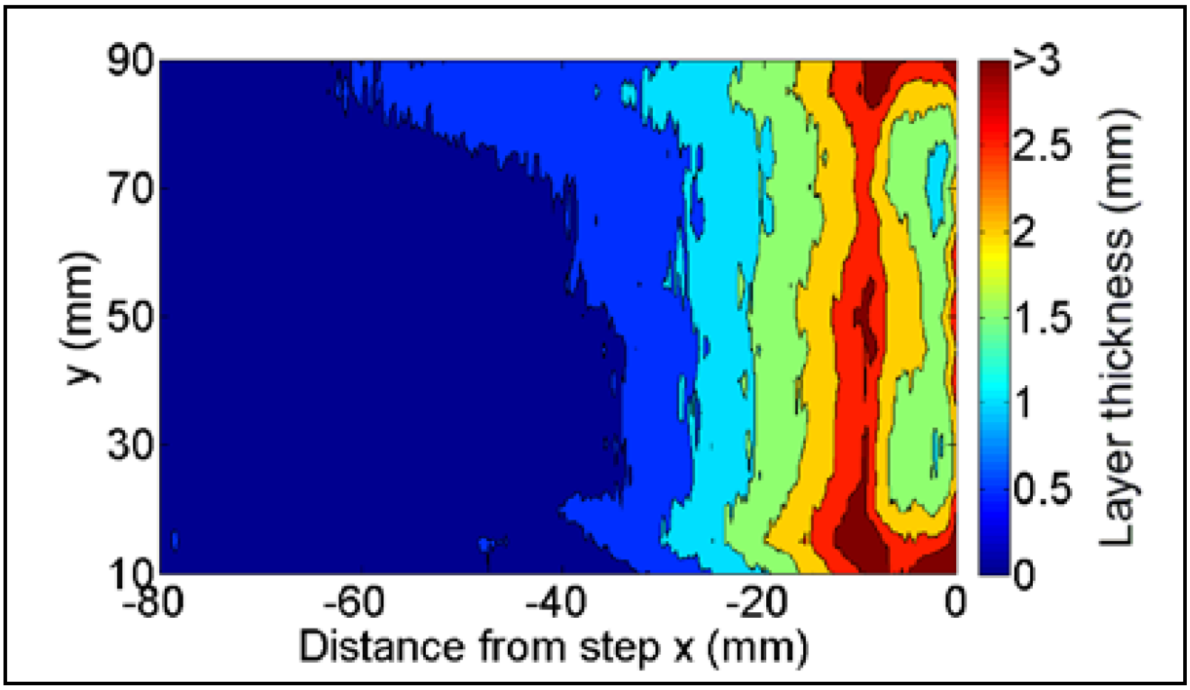

Figure 9 Layer thickness in front of the FFS after 54 min deposition time at Re_s = 4190

The layer height is nearly symmetric to the midplane of the channel. In front of the obstacle is a very high deposit followed by a region with nearly no settled dust. The very high deposit is caused by the impaction of the particles with the forward facing step. The change of the flow velocity vector in front of the step is very high such that the particles cannot follow the flow, resulting in their collision with and adhesion to the obstacle. Simultaneously a change in the flow field occurs. Schematically the effect is shown in Figure 10. By rotating the part of the step at which particles adhered it was possible to remove the section with the impact layer and measure the height of the deposited dust on the entire FFS. These measurements confirmed that beneath the impact layer, in the recirculation region, the floor was virtually dust-free as illustrated in Figure 10.

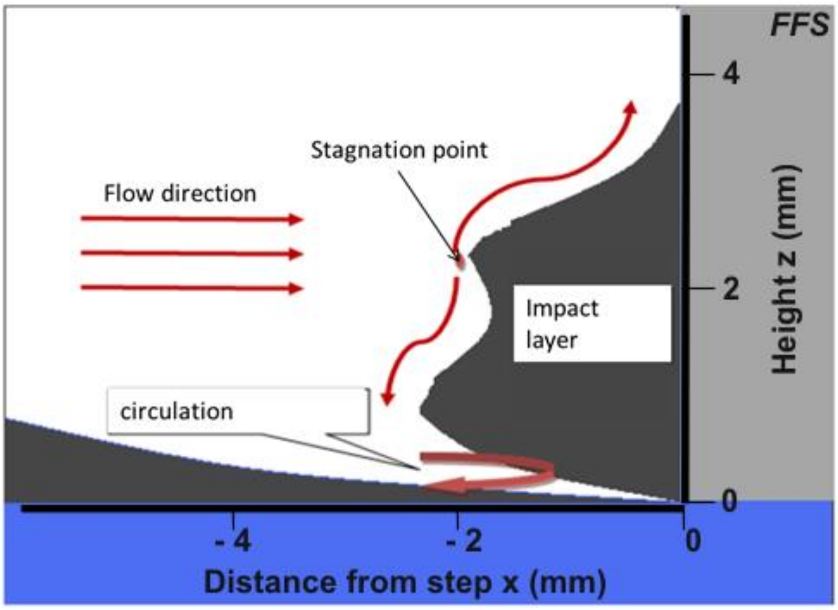

Figure 10 Dust deposits (schematically drawn in dark grey) on the channel bottom and adhering to the front of the FFS (light grey) with schematically illustrated change of the flow field

Figure 11 shows the multilayer height averaged over the channel width for the three different time steps at Re_s = 4190. The layer grows nearly linearly over the time intervals with a characteristic hill-valley-region in front of the step and is qualitatively comparable to the layers created at all the other Reynolds numbers tested.

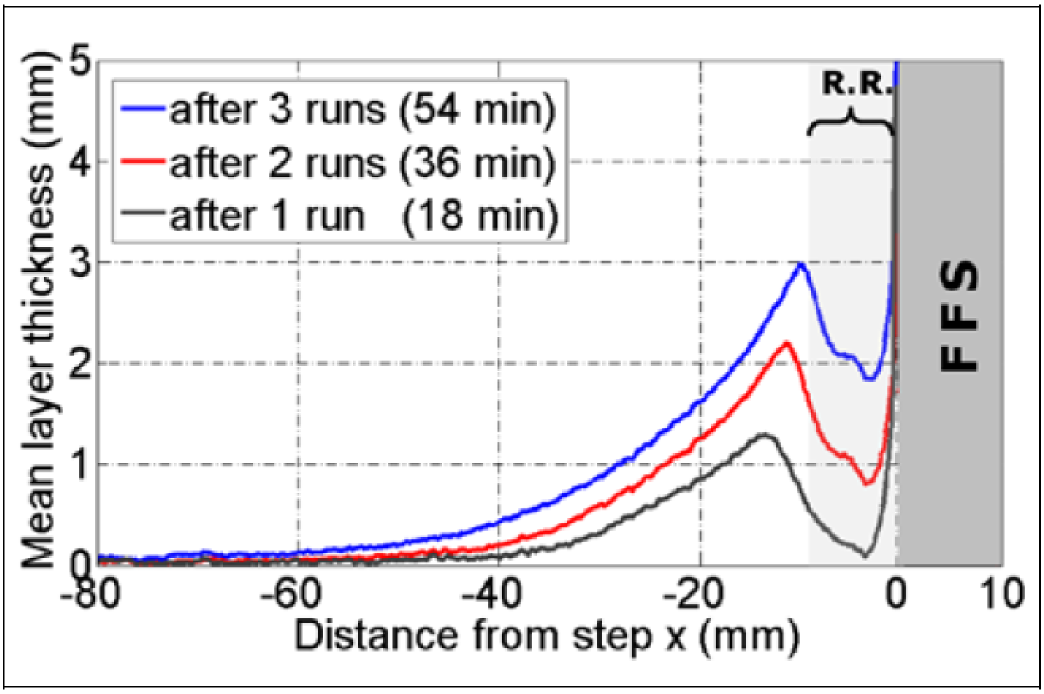

Figure 11 Layer height averaged over the channel width at a Re_s = 4190 at different time steps

By integrating the data points of the height over the scanned area the deposited volume could be calculated. Figure 12 illustrates the obtained results depending on time and Reynolds number.

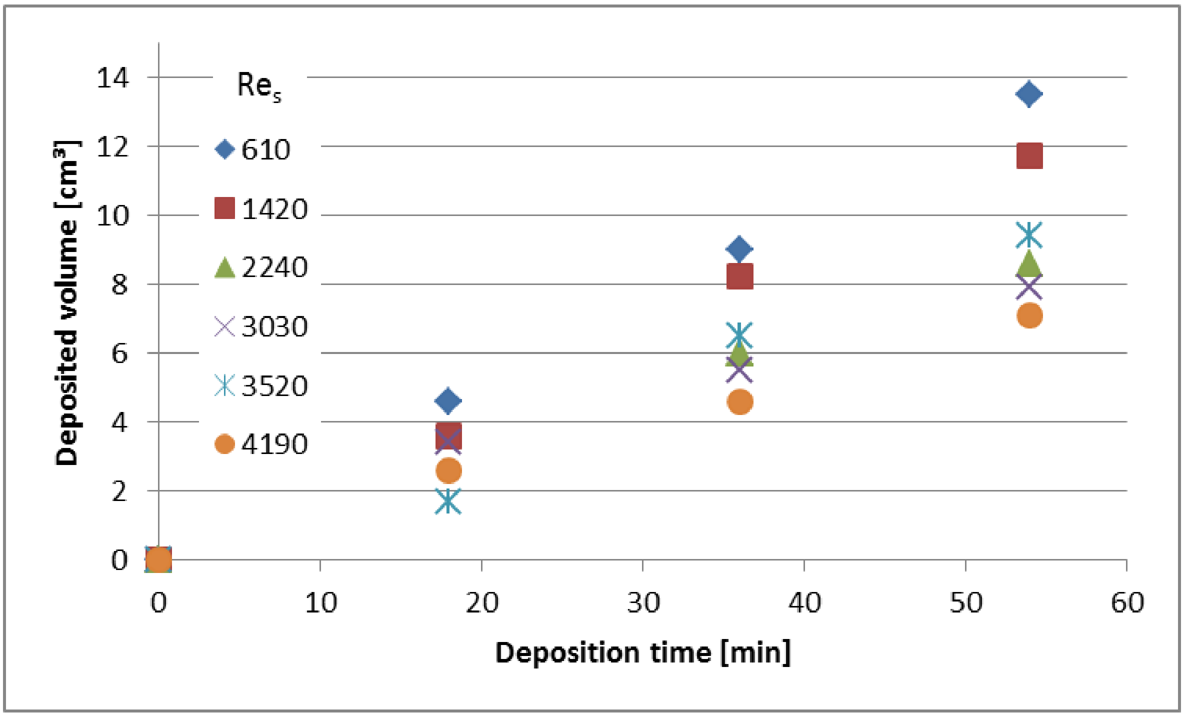

Figure 12 Deposited dust volume in front of the step depending on Reynolds number and deposition time

Figure 12 confirms the nearly constant deposition velocity of the graphite dust. Additionally a decrease of deposited volume with increasing Reynolds number could be found.
By removing the graphite layer after the last run and determining its mass gravimetrically, the density of the deposit could be calculated. For different Reynolds numbers the mass of the settled dust m_d and the density ρ_d are listed in Table 5.

Table 5 Mass and resulting powder density of the deposited dust at different Reynolds numbers

Re	m_d [g]	ρ_d [g/cm³]
610	3	0.22
1420	2.8	0.24
3030	2.2	0.28
4190	2.3	0.33

As shown the mean density increases with increasing Re. In comparison, the maximum density for stamped dust was determined to be about 0.76 g/cm³ and therefore the settled dust reaches 29 % to 43 % of the maximum achievable density. Using Eq. 6 for calculation of the deposition velocity based on particle concentration in the fluid and mass of the settled dust after the 3 runs a nearly linear correlation of Re with the deposition velocity could be identified as shown in Figure 13.

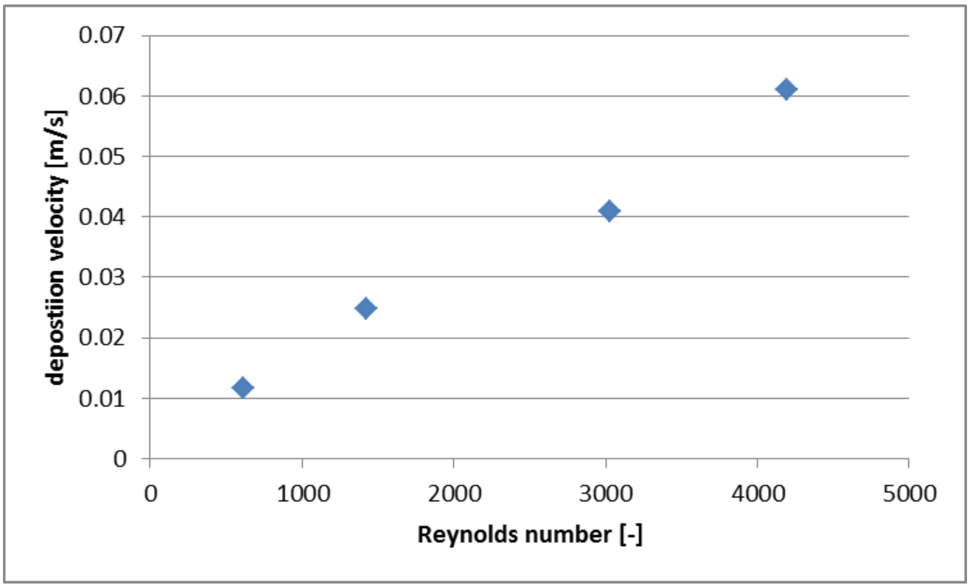

Figure 13 Particle deposition velocity depending on the step height based Reynolds number

4 Conclusion

The deposition of graphite dust in a flow channel with and without flow obstacle was investigated. Aim of this work was to characterize the particle deposition behaviour of graphite particles under conditions relevant for HTR primary circuits. Originally, graphite particles produced by the test facility *pebble mill* should have been used for these experiments. However, the amount of particles generated by the pebble mill did not suffice as supply for the experiments. Therefore, an industrial graphite powder with characteristics similar to the graphite dust found in the THTR reactor was used instead. The experiments were performed within a small open loop flow channel with air at ambient conditions to ensure comparability of the dimensionless characteristic numbers with those of a HTR primary circuit atmosphere. Other influences such as humidity, oxygen influence, or any temperature-related transport mechanisms were not taken into account. The comparison of the particle size distribution of dispersed dust with that deposited as a single layer on a flat plate showed an increase of the mean particle size suggesting larger particles are more susceptible to deposition.

The creation of multilayer deposits in front of a forward facing step was observed as well. Previously, a flow field characterization by means of particle image velocimetry was conducted revealing a recirculation area in front of the obstacle with size and flow characteristics depending on the Reynolds number. By use of a laser triangulation system a nearly constant growth velocity of the particle layer was observed. By gravimetrical weighing of the dust deposit the particle deposition velocity and the density of the deposit could be calculated. It was found that the deposition velocity increased almost linearly with the Reynolds number. Simultaneously, the density of the layer increased, while the volume decreased.

5 Literature

[1] **Ziermann, E., Ivens, G.:** *Abschlußbericht über den Leistungsbetrieb des AVR-Versuchskraftwerkes*, Report 3448, Forschungszentrum Jülich GmbH, 1997

[2] **Stempniewicz, M.M., Winters, L., Caspersson, S.A.:** *Analysis of dust and fission products in a pebble bed NGNP*, Nuclear Engineering and Design 251 (2012), 433-442.

[3] **Schreier M.; Lustfeld M.; Lippmann W.; Hurtado A.:** *Graphite Dust Production and Characterisation*, ARCHER Deliverable D23.23, TU Dresden, 2014

[4] **Rott; Wahsweiler H. G.:** *Abschlussbericht zum Vorhaben Auswertung von Inbetriebnahmeereignissen am THTR-300 für HTR-Nachfolgeanlagen. Teilvorhaben 6.1: Verteilung und Auswirkung von Graphitstaub im Primärkreis,* HRB-Berichte BA 5898, Mannheim, 1990

[5] **Hinds, W. C.:** *Aerosol Technology: Properties, behavior and measurement of airborne particles, 2nd edition*, John Wiley & Sons Inc., New York, 1999

[6] **Sehmel, G. A.:** *Particle Eddy Diffusivities and Deposition Velocities for Isothermal Flow and Smooth Surfaces*, Journal of Aerosol Sciences Vol. 4, 1973

[7] **Fachinger, J.; Kummer, A.; Koster, A.; Caspary, G.; Makumbe, M.; Barnert, H.; Seubert, M.; Naicker, L.:** *Examination of Dust in AVR pipe components. HTR2008-58033*, Proceedings of the 4th International Topical Meeting on High Temperature Reactor Technology, HTR2008, Washington DC, USA, 2008

[8] **Sherry, M.; Jacono, D. L.; Sheridan, J.:** *An experimental investigation of the recirculation zone formed downstream of a forward facing step*, Journal of wind engineering and industrial aerodynamics 98 (2010), 888 - 894

6 Annex: Document approval by beneficiaries' internal QA

Fill involved beneficiaries as appropriate (mandatory for Milestones and Deliverables, but optional for other document type)

#	Name of beneficiary	Approved by	Function	Date
1				
2				
3				
4				
6				
7				
8				
9				
10				
11				
12				
13				
14				
15				
16				
17				
18				
19				